Global and Planetary Change 88–89 (2012) 1–9

Contents lists available at SciVerse ScienceDirect

Global and Planetary Change

journal homepage: www.elsevier.com/locate/gloplacha

Variability and extremes of northern Scandinavian summer temperatures over the past two millennia

Jan Esper [a,*], Ulf Büntgen [b], Mauri Timonen [c], David C. Frank [b,d]

[a] Department of Geography, Johannes Gutenberg University, 55099 Mainz, Germany
[b] Swiss Federal Research Institute WSL, 8903 Birmensdorf, Switzerland
[c] Finnish Forest Research Institute, Rovaniemi Research Unit, 96301 Rovaniemi, Finland
[d] Oeschger Centre for Climate Change Research, University of Bern, Switzerland

ARTICLE INFO

Article history:
Received 22 October 2011
Accepted 16 January 2012
Available online 24 January 2012

Keywords:
climate variability
Palaeoclimate
Common Era
tree-rings
Scandinavia

ABSTRACT

Palaeoclimatic evidence revealed synchronous temperature variations among Northern Hemisphere regions over the past millennium. The range of these variations (in degrees Celsius) is, however, largely unknown. We here present a 2000-year summer temperature reconstruction from northern Scandinavia and compare this timeseries with existing proxy records to assess the range of reconstructed temperatures at a regional scale. The new reconstruction is based on 578 maximum latewood density profiles from living and sub-fossil *Pinus sylvestris* samples from northern Sweden and Finland. The record provides evidence for substantial warmth during Roman and Medieval times, larger in extent and longer in duration than 20th century warmth. The first century AD was the warmest 100-year period (+0.60 °C on average relative to the 1951–1980 mean) of the Common Era, more than 1 °C warmer than the coldest 14th century AD (−0.51 °C). The warmest and coldest reconstructed 30-year periods (AD 21–50 = +1.05 °C, and AD 1451–80 = −1.19 °C) differ by more than 2 °C, and the range between the five warmest and coldest reconstructed summers in the context of the past 2000 years is estimated to exceed 5 °C. Comparison of the new timeseries with five existing tree-ring based reconstructions from northern Scandinavia revealed synchronized climate fluctuations but substantially different absolute temperatures. Level offset among the various reconstructions in extremely cold and warm years (up to 3 °C) and cold and warm 30-year periods (up to 1.5 °C) are in the order of the total temperature variance of each individual reconstruction over the past 1500 to 2000 years. These findings demonstrate our poor understanding of the absolute temperature variance in a region where high-resolution proxy coverage is denser than in any other area of the world.

1. Introduction

Millennial-length temperature reconstructions became an important source of information to benchmark climate models (IPCC, 2007), detect and attribute the role of natural and anthropogenic forcing agents (Hegerl et al., 2006), and quantify the feedback strength of the global carbon cycle (Frank et al., 2010b). Newer approaches are using palaeoclimatic reconstructions to assess the likelihood of simulation ensemble members, and thus help to constrain future climate scenarios (Yamazaki et al., 2009). These efforts are, however, limited by the number of high quality reconstructions and their ability to properly quantify the absolute range of past temperature variations (Esper et al., 2002), adding considerable uncertainty to hemispheric scale reconstructions that combine multiple regional proxy records (Frank et al., 2010a). At this point, we seem to have a fairly good understanding of the course of temperature change over the past millennium, i.e. the Medieval Warm Period (MWP), cooling into the Little Ice Age (LIA), and subsequent warming into the 20th century. However, the absolute variance (or amplitude) of temperature change (in degrees Celsius) is more poorly constrained, and might range from less than 0.5 °C to more than 1 °C over the past 1000 years at hemispheric scales (Frank et al., 2010b and references therein). The situation is even less clear prior to medieval times, as only few high-resolution reconstructions are available for the Common Era (Jones et al., 2009) complicating assessments of the absolute temperature amplitude during the Roman and subsequent Migration periods (Büntgen et al., 2011).

While discrepancies in hemispheric scale reconstructions have received considerable attention over the past decades (Frank et al., 2010a), less debate has been centred on the uncertainties of regional reconstructions and their abilities to properly estimate the evolution and amplitude of temperatures over the past centuries to millennia. This is surprising for a variety of reasons including the fact that large-scale reconstructions are often a simple aggregation of these regional reconstructions. It should thus be clarified how large errors at

* Corresponding author. Tel.: +49 6131 3922296; fax: +49 6131 3924735.
E-mail address: esper@uni-mainz.de (J. Esper).

0921-8181/$ – see front matter © 2012 Published by Elsevier B.V.
doi:10.1016/j.gloplacha.2012.01.006

the regional level may be, and how these regional errors contribute to large-scale uncertainties.

Northern Scandinavia is one of the core regions from where multiple tree-ring based summer temperature reconstructions spanning the past 1–2 millennia are available (overview in Gouirand et al., 2008). The most widely cited (and integrated in hemispheric scale reconstructions) of these records is the timeseries derived from tree-ring maximum latewood densities (MXD) from the Tornetraesk region in northern Sweden (Schweingruber, 1988, updated in Grudd, 2008). Reasons for this extensive consideration include the length of the reconstruction (back to AD 500), as well as the robust climate signal of MXD data (correlation against summer temperatures typically >0.7) that is generally stronger than for traditional tree-ring width (TRW) data (typically <0.5). The Tornetraesk MXD data have also been combined with TRW data from the same trees to form an alternative reconstruction reaching back to AD 500 (Briffa et al., 1992). Since then, three additional reconstructions from Fennoscandia have been developed – all based on TRW, spanning the past two millennia, but partly relying on the same raw measurement series (Grudd et al., 2002; Briffa et al., 2008; Helama et al., 2010) – so that multiple, independently developed records can be used to assess the variability of summer temperatures over the past 1500 to 2000 years at a regional scale.

We here address this issue by *(1)* introducing a new summer temperature reconstruction that is longer and much better replicated than any other published MXD-based record, *(ii)* using this timeseries to derive estimates of the absolute range of regional summer temperature variation considering extremely cold and warm reconstructed years and periods over the past two millennia, *(iii)* comparing these estimates with existing tree-ring based reconstructions, and finally *(iv)* using the differences among these various records to assess the uncertainty of reconstructed temperatures within a confined region.

2. Material and Methods

We developed 587 high-resolution density profiles (Frank and Esper, 2005) from living and sub-fossil *Pinus sylvestris* in northern Sweden and Finland to form a long-term MXD record (N-Scan) spanning the 138 BC to AD 2006 period (Table 1). The living-tree samples were obtained from pines growing at the shores of three lakes to ensure data homogeneity with the sub-fossil samples obtained from 14 lakes in the region (Fig. 1). Spatial data homogeneity was assessed using a total of nine *Pinus sylvestris* MXD chronologies from northern Sweden, Finland, and Russia ($r_{1812\text{-}1978} = 0.72$; not shown) validating the integration of data throughout the region (Eronen et al., 2002). All MXD measurements were derived from high-precision X-ray radiodensitometry (Schweingruber et al., 1978).

Table 1
Living-tree and sub-fossil pine sites integrated in the long-term N-Scan reconstruction.

	Location	Lon.	Lat.	No. Series	Start	End
Living	Ket	24.05	68.22	49	1596	2006
	Kir	20.10	67.90	87	1656	2006
	Tor	19.80	68.20	79	1800	2006
Sub-fosssil	Aka	24.20	67.70	8	1311	1782
	Hae	27.50	67.50	2	1342	1533
	Hal	29.00	66.80	6	691	1282
	Kal	24.80	68.50	10	271	1553
	Koi	27.50	68.70	10	–47	1767
	Kol	29.00	66.80	6	1686	1916
	Kom	28.00	68.50	83	–215	1906
	Kul	23.00	68.50	49	488	1704
	Luo	28.00	68.50	68	-4	1897
	Nak	23.50	68.70	37	372	1822
	Pel	24.80	68.50	5	171	1743
	Pet	27.00	69.50	10	883	1792
	Pit	27.50	67.50	16	–6	1749
	Rie	28.00	68.50	59	301	1770

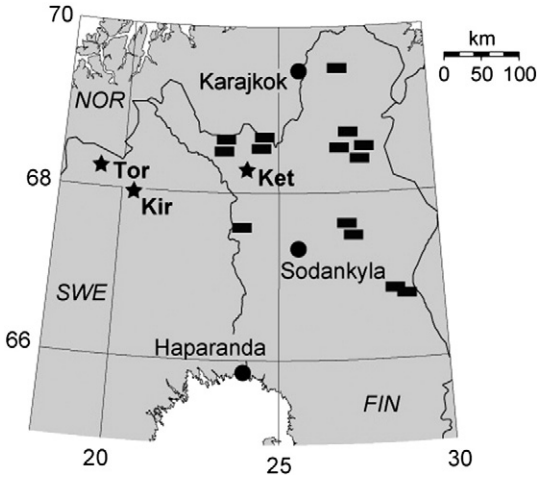

Fig. 1. Map showing the three living-tree (stars) and 14 sub-fossil (rectangles) pine sites integrated in the N-Scan record, together with the long-term meteorological stations in Haparanda, Karasjok, and Sodankyla (circles).

Biological age trends inherent to the MXD data were removed using RCS (Esper et al., 2003), a detrending method that preserves high-to-low frequency variance in the resulting indices. MXD series were combined using the arithmetic mean. Variance changes, such as those that can arise from temporally changing replication and inter-series correlation (Frank et al., 2007), were adjusted. The new MXD record was calibrated against mean JJA temperatures derived from the long-term instrumental stations in Haparanda, Karasjok, and Sodankyla (Fig. 1) over the 1876–2006 period, and transferred into summer temperature estimates using ordinary least squares (OLS) regression (with MXD as the dependent variable) (Cook and Kairiukstis, 1990).

N-Scan was used to identify temperature extremes over the 138 BC to AD 2006 period including exceptionally cold and warm summers, 30-year periods, and centuries. The 30-year periods were additionally considered for comparison with existing temperature reconstructions from the region, including a combined TRW-plus-MXD record by Briffa et al. (1992) from northern Sweden (hereafter Briffa92), a TRW-based record by Grudd et al. (2002) from northern Sweden (hereafter Grudd02), a TRW-based record by Briffa et al. (2008) from northern Finland and Sweden (hereafter Briffa08), a MXD-based record by Grudd (2008) from northern Sweden (hereafter Grudd08), and a TRW-based record from Helama et al. (2010) from northern Finland (hereafter Helama10). Of the six reconstructions considered here, four reach back to AD 1 and earlier (N-Scan, Grudd02, Briffa08, Helama10), and two back to AD 500 (Briffa92, Grudd08). Whereas some of these records share data (e.g. Briffa92 and Grudd02, Briffa92 and Grudd08,) others are fully independent (e.g. Grudd02 and Helema10). All records were, however, independently derived and as such individually treated and considered in large-scale reconstructions. Due to data overlap, uncertainties defined by the spread amongst reconstructions should be considered as conservative estimates.

Temperature differences among the various proxy records were assessed after re-calibrating each of the six reconstructions against JJA temperatures over the common 1876–1993 period (except for the Briffa92 record that only extends until 1980) and transferring the records into summer temperatures using OLS regression with the tree-ring data as the independent variable. These calibrated and transferred timeseries were used to calculate the range of reconstructed temperatures during extremely cold and warm years. We also smoothed the six proxy records using 30-year filters prior to the calibration against JJA temperatures (over the 1891–1979 period) and analyzed the difference between the reconstructions during

extremely cold and warm 30-year periods. This additional approach provides some insight into the effects of calibration procedure on the absolute amplitude of reconstructed temperatures, though these methodological uncertainties are not the focus of this current study (see for example Esper et al., 2005; Lee et al., 2008).

3. Results

3.1. Summer temperatures derived from N-Scan

The N-Scan chronology contains multi-decadal to centennial scale fluctuations superimposed on a long-term negative trend over the past two millennia (Fig. 2). The number of single MXD measurement series integrated in this record changes considerably through time, from only 5 series before 46 BC to 11 series in AD 1 and 197 series in AD 2001. Mean chronology age calculated for each year over the 138 BC – AD 2006 period is, however, fairly balanced throughout time, largely due to the integration of samples from various lakes and consideration of samples from relatively young living trees from lakeshores. Coherency among the single MXD measurement series, expressed by the inter-series correlation, is fairly high (mean *Rbar* = 0.43) and temporally robust indicating capability of the N-Scan record to reconstruct high-resolution climate variations over longer timescales.

Calibration against regional climate data indicated the N-Scan record to contain a significant JJA temperature signal ($r^2_{1876\text{-}2006} = 0.59$; Fig. 3). The signal is temporally stable as revealed by split period calibration/verification statistics ($r^2_{1876\text{-}1941} = 0.61$, $r^2_{1942\text{-}2006} = 0.57$) suggesting that the record does not suffer from biases reported from other tree-ring sites in Northern Hemisphere high latitude environments (D'Arrigo et al., 2008; Esper and Frank, 2009; Esper et al., 2010). We also assessed the significance of the earlier, less replicated periods of N-Scan record by re-calculating RCS chronologies 2000 times using subsamples of living trees (Fig. 3B). These tests revealed that the JJA temperature signal is robust down to a replication of 10 MXD measurement series ($r > 0.70$), which appeared as an informative metric when analysing and interpreting N-Scan fluctuations during the first centuries AD where replication is substantially reduced.

The calibrated and transferred MXD record shows considerable summer temperature variations over the past two millennia (Fig. 4), with the five warmest reconstructed summers deviating on average by 2.25 °C from the 1951–80 mean, and the five coldest summers by −2.79 °C (Table 2). Four out of the five warmest summers occurred

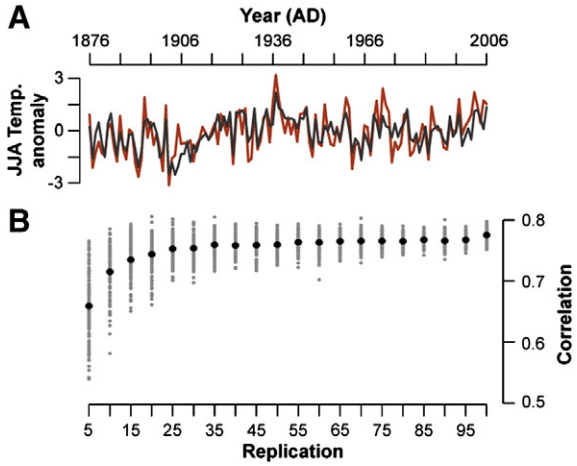

Fig. 3. Calibration of the long-term N-Scan record. (**A**) N-Scan (grey curve) regressed against regional JJA temperatures (red curve) over the 1876–2006 period (proxy as the dependent variable, $r^2 = 0.59$). (**B**) Multiple Pearson correlation coefficients derived from calibrating a total of 2000 RCS chronologies against JJA temperatures (1876–2006 period). The RCS chronologies were developed using 5, 10, 15, …, 100 MXD series randomly drawn from the population of living trees (215 series, see Table 1) in conjunction with the full relict population (372 series).

at the beginning of the reconstruction period during Roman times, and the majority of extremely cold summers were recorded during the second millennium AD – a feature that is associated with a millennial scale cooling trend related to slow changes in boreal summer orbital forcing (Berger and Loutre, 1991). Consequently, the 1st century AD is the warmest 100-year period (+ 0.60 °C), and the succession of cold and warm centuries over the past 2000 years provides clear indication of warmth during Roman and Medieval times alternating with cool conditions during the mid first and second millennium, the Migration and Little Ice Age periods. The five warmest centuries, all recorded during the first millennium AD, were on average > 0.80 °C warmer than the five coldest centuries of the past two millennia (Table 2).

For an assessment of the most exceptional deviations in these key periods, we highlighted the warmest 30-year periods during Roman (AD 27–56), Medieval (918–947), and Modern (AD 1918–1947) times, as well as the coldest periods during Migration (AD 299–328) and Little Ice Age (AD 1453–1482) times (see the grey bars in Fig. 4). These periods were then considered for the comparison

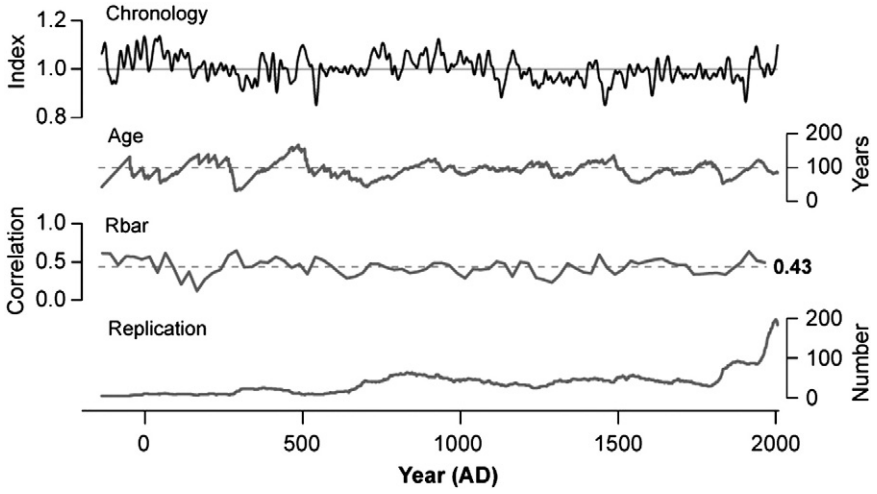

Fig. 2. RCS-detrended N-Scan chronology shown together with the mean chronology age, Rbar, and replication curves. The chronology has been smoothed using a 20-year filter. Chronology age and replication were calculated for each year since 138 BC, and inter-series correlation (Rbar) over 50-year periods shifted stepwise by 25 year along the chronology.

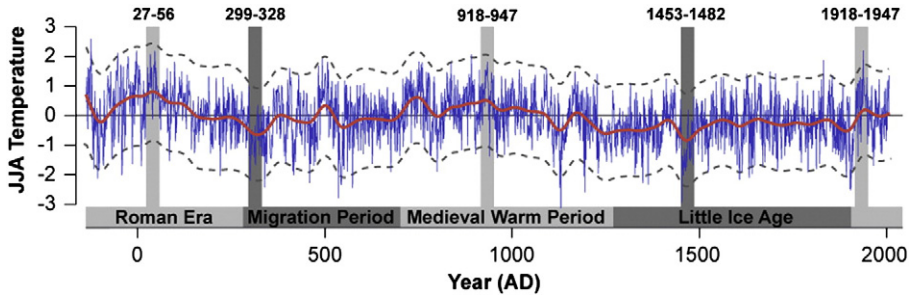

Fig. 4. Northern Scandinavian JJA temperatures back to 138 BC. The annually resolved N-Scan record (blue curve) shown together with 100-year filters of the reconstruction (red curve) and uncertainty estimates integrating standard and bootstrap errors (dashed curves). Light and dark grey bars indicate exceptionally warm and cold 30-year periods during the Roman, Migration, Medieval Warm, Little Ice Age, and Modern Warm Periods. Temperatures are expressed as anomalies with respect to the 1951–1980 mean.

of reconstructed summer temperatures among six regional proxy records.

3.2. Summer temperatures derived from six regional reconstructions

Calibration against instrumental climate data revealed significant JJA temperature signals in all high-resolution proxy records considered here (Fig. 5). Correlations are generally lower for the TRW-based records ($r_{1876\text{-}1993} = 0.45\text{-}0.54$; Grudd02, Helama10, Briffa08) than for MXD-based records ($r_{1876\text{-}1993} = 0.71\text{-}0.77$; Grudd08, Briffa92, N-Scan). These differences affect the variance of reconstructed temperatures when using regression-based calibration techniques as applied here (Esper et al., 2005), i.e. the reconstruction variance is directly related to the unexplained variance of the regression model (see the grey and red curves in Fig. 5A). This bias is reduced when smoothing the data before calibration, as correlations with instrumental data increase to $r_{1891\text{-}1979} > 0.89$ for most records, i.e. unexplained variance is small. Of the proxy records considered here, only the Grudd08 timeseries indicates an obvious mismatch with recent JJA temperatures (Fig. 5B) constraining the correlation of this record to only $r = 0.84$, and consequently reducing the reconstructed temperature variance towards lower values relative to the other records.

The two calibration schemes result in slightly differing arrangements of proxy records over the Common Era, though the general order (e.g. warmest temperatures reconstructed by Grudd08, coolest by Grudd02 and Briffa08, etc.) remain unaffected (Fig. 6). The average correlation among the reconstructions over the AD 500–1980 common period is $r = 0.51$ for the 30-year smoothed and $r = 0.54$ for the unsmoothed timeseries. Whereas these metrics underscore coherence among the reconstructions – a feature also obvious from visual inspection of Fig. 6 – the compilation of timeseries in one plot also emphasize the sizeable differences in absolute temperature levels reconstructed over the past two millennia: Grudd08 indicates warmest reconstructed temperatures, frequently > 1 °C warmer than Briffa08 and Grudd02 both indicating coolest temperatures throughout most of the past 2000 years. The other records appear in between these extremes, except for the first 500 years of Common Era when N-Scan showed highest values.

To add detail on the ensemble variance, we plot and analyse the temperature ranges among the reconstructions during exceptionally warm and cold 30-year periods (Fig. 7). This approach revealed differences in reconstructed summer temperatures ranging from 0.4 °C during the warmest 30-year period in the 20th century (AD 1918–47) up to 1.6 °C during the warmest Medieval period AD 918–947. These differences are particularly striking as the timeseries analyzed here are all highly correlated ($r > 0.84$) at inter-annual and inter-decadal (30-year smoothed) scales, and some of the records even share data, such as Briffa92 and Grudd08, or Briffa08 and Grudd02. The differences among records that are derived from (partly) the same input data (i.e. same measurements and/or different measurements from the same trees) underscore the importance of measurement protocols, and data processing and chronology development techniques on the shape of the final reconstructions. The 0.4 °C uncertainty during the 20th century itself is already sizeable but is more tightly constrained due to the calibration with the instrumental data.

Analysis of the coldest and warmest reconstructed summers revealed temperatures differences ranging from 1.2 °C in AD 536 – a year characterized by a strong cooling across the globe following a large volcanic eruption (D'Arrigo et al., 2001) – up to 3.0 °C in AD 891 (Fig. 8). These among-reconstruction differences are in the same order than the temperature variance of the individual records over the Common Era (see Figs. 4 and 6). For example, temperature

Table 2
Summer temperature deviations in the five coldest and warmest years and centuries since 138 BC derived from N-Scan.

Rank	Year	Temperature deviation	Century	Temperature deviation
1.	125 BC	2.59 °C	1st	0.60 °C
2.	AD1937	2.19 °C	8th	0.37 °C
3.	4 BC	2.18 °C	1st (BC)	0.37 °C
4.	AD 46	2.17 °C	9th	0.30 °C
5.	54 BC	2.11 °C	10th	0.30 °C
Mean		**2.25 °C**		**0.39 °C**
1.	AD 1130	−3.12 °C	14th	−0.51 °C
2.	AD 1453	−2.94 °C	13th	−0.49 °C
3.	AD 536	−2.78 °C	15th	−0.45 °C
4.	AD 1194	−2.58 °C	4th	−0.39 °C
5.	AD 1904	2.51 °C	18th	−0.31 °C
Mean		**−2.79 °C**		**−0.43 °C**

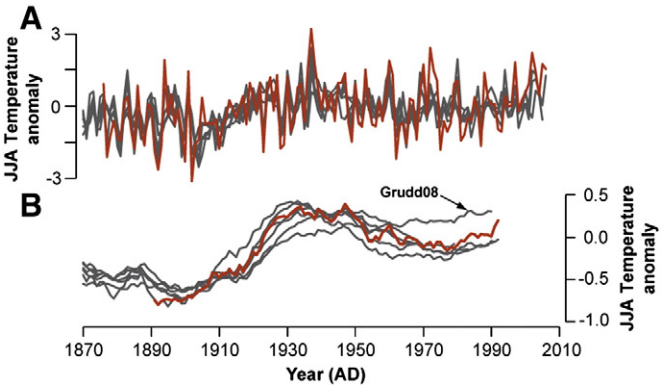

Fig. 5. Calibration of northern Scandinavian tree-ring chronologies against regional climate data. (A) OLS regression of the N-Scan, Briffa92, Grudd02, Briffa08, Grudd08, and Helama10 timeseries (grey curves) against mean JJA temperatures recorded in Haparanda, Karasjok, and Sodankyla (red curve) over the 1876–1993 period. (B) The same data but first smoothed using a 30-year moving average and then regressed against regional JJA temperatures over the 1891–1979 period. All temperatures expressed as anomalies from the 1951–1980 mean.

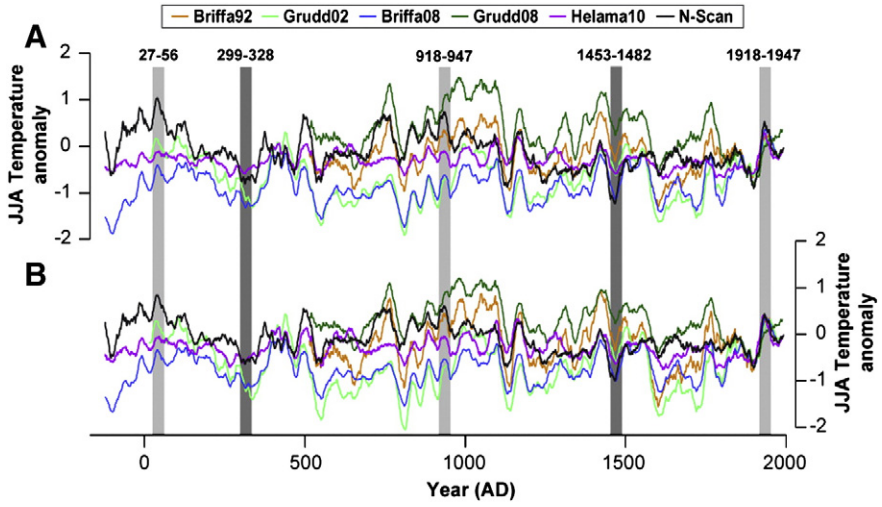

Fig. 6. Northern Scandinavian summer temperatures derived from six tree-ring based reconstructions from northern Sweden and Finland. (A) All records were calibrated against regional JJA temperatures over the 1876–1993 period (Briffa92 ends in 1980) using OLS regression. (B) The same records but first smoothed using a 30-year moving average and then regressed against JJA temperatures over the 1889–1979 period.

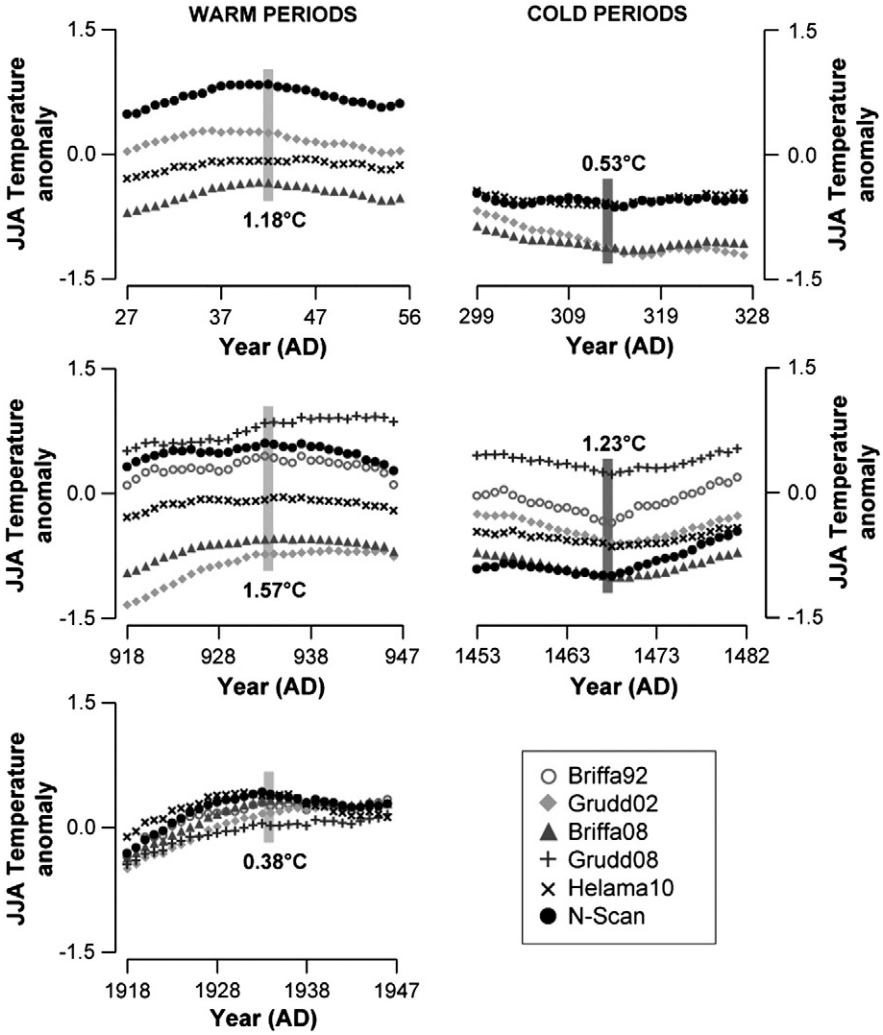

Fig. 7. Temperature range among regional reconstructions. Symbols indicate 30-year moving averages of six tree-ring based summer temperature reconstructions during exceptionally cold and warm periods of the past two millennia as derived from the N-Scan reconstruction (see grey bars in Figs. 4 and 6). Grey bars highlight the temperature ranges among the reconstructions over the AD 27–56, 299–328, 918–947, 1453–1482, and 1918–1947 periods. All records have been smoothed and then regressed against instrumental summer temperatures over the 1891–1979 period (see Fig. 6B).

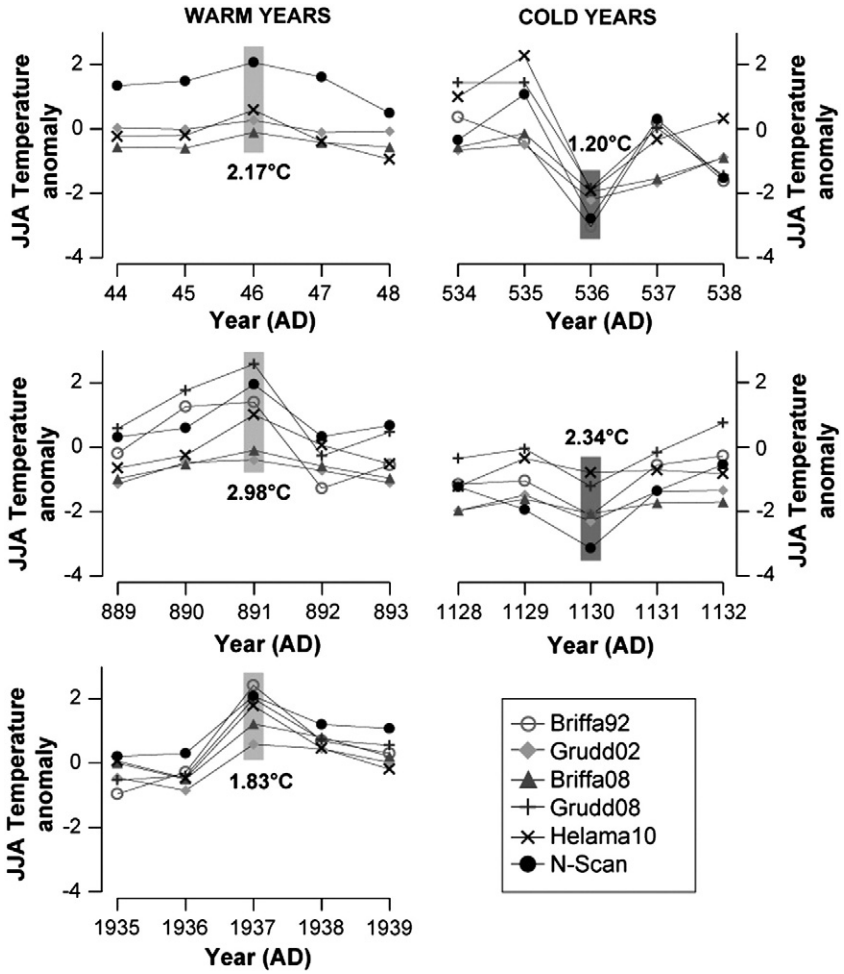

Fig. 8. Temperature range among regional reconstructions. Symbols indicate six tree-ring based summer temperature reconstructions in exceptionally cold and warm years (in the centre of each panel together with two previous and following years) of the past two millennia as derived from the N-Scan reconstruction (see Table 2). Grey bars highlight the temperature range among the reconstructions in these years AD 46, 536, 891, 1130, and 1937. All records have been regressed against instrumental summer temperatures over the 1876–1993 period (see Fig. 6A).

variance of the N-Scan record, approximated through the difference between the 30 coldest (−2.27 °C) and warmest (+1.65 °C) summers of the past 2000 years (Table 3) is 3.9 °C (see the dashed lines in Fig. 9). The distributions of values from all proxy records during these years are, however, fairly flat and even overlap between −1.5 and +1.76 °C (grey bars in the centre of Fig. 9), again emphasizing the uncertainties among reconstructions in exceptionally cold and warm years.

4. Discussion and Conclusions

The MXD-based summer temperature reconstruction presented here sets a new standard in high-resolution palaeoclimatology. The record explains about 60% of the variance of regional temperature data, and is based on more high-precision density series than any other previous reconstruction. Importantly, MXD sample replication prior to the Little Ice Age, during Medieval times and throughout the first millennium AD, is much better than in any other record, and we demonstrated – based on calibration trials using reduced datasets – that these early sections of the N-Scan record likely still contain useful climate information. This persistent climate signal allowed an estimation of temperature variability throughout the Common Era, revealing warmth during Roman and Medieval times were larger in extent and longer in duration than 20th century conditions.

According to this new record, summer temperatures varied by 1.1 °C among the 14th and 1st centuries, the coldest and warmest 100-year periods of the past two millennia. Temperatures ranged by more than 5 °C among the five coldest and warmest summers of the past 2000 years. These estimates are, however, related to the approach used for proxy transfer, i.e. figures would change, if the calibration method, period, and/or target were modified (Frank et al., 2010b). For example, variance among the 30 coldest and warmest N-Scan summers (Table 3) increases from 3.92 °C to 5.79 °C, if scaling (i.e. adjustment of the mean and variance) instead of OLS regression is used for proxy transfer. These differences between scaling- and regression-based approaches are proportional to the unexplained variance of the calibration model (Esper et al., 2005), and we suggest smoothing the proxy and instrumental timeseries prior to calibration, as this procedure decreases the unexplained variance in all Scandinavian tree-ring records and thus minimizes the differences between various calibration methods (Cook et al., 2004).

Our results, however, also showed that these methodological uncertainties are dwarfed by the variance among the individual reconstructions. Differences among six northern Scandinavian tree-ring records are > 1.5° in 30-year extreme periods and up to 3 °C in single extreme years, a finding we didn't expect, as the proxy records: *(i)* all calibrate well against regional instrumental data, *(ii)* partly share the same measurement series (or use differing parameters – TRW and MXD – from the same trees), and *(iii)* originate from a confined region in northern Scandinavia that is characterized by a homogeneous

Table 3
Thirty coldest and warmest reconstructed summers since 138 BC derived from N-Scan, together with the corresponding JJA temperatures from Briffa92, Grudd02, Briffa08, Grudd08, and Helama10.

	Year	Rank	N–Scan	Briffa92	Grudd02	Briffa08	Grudd08	Helama10
30 coldest years	1130	1.	−3.13	−2.11	−2.29	−2.06	−1.20	−0.79
	1453	2.	−2.95	−2.39	−0.82	−1.34	−1.34	−1.04
	536	3.	−2.79	−3.04	−2.20	−1.95	−1.84	−1.92
	1194	4.	−2.60	−1.80	−1.20	−1.27	−1.28	−0.36
	1904	5.	−2.53	−2.35	−1.82	−1.60	−2.37	−0.90
	1902	6.	−2.49	−2.45	−0.35	−0.77	−2.03	−0.72
	574	7.	−2.46	−2.64	−0.81	−0.93	−1.90	−0.34
	1127	8.	−2.45	−1.61	−1.19	−1.41	−0.86	−0.37
	339	9.	−2.44		−1.53	−1.61		−0.93
	543	10.	−2.36	−1.39	−1.77	−1.87	−0.77	−1.04
	1363	11.	−2.34	−1.69	−1.00	−1.44	−1.06	−0.94
	544	12.	−2.33	−1.80	−2.42	−2.18	−0.72	−0.94
	1349	13.	−2.30	−1.30	−1.73	−1.67	−0.88	−1.05
	459	14.	−2.29		−1.17	−1.31		−0.73
	301	15.	−2.21		−0.43	−0.97		−0.47
	1607	16.	−2.19	−1.85	−1.95	−1.86	−0.98	−1.25
	1633	17.	−2.13	−2.40	−1.36	−1.26	−1.79	−1.03
	1892	18.	−2.12	−2.43	−0.74	−1.21	−1.75	−1.08
	1192	19.	−2.07	−0.97	−0.67	−0.98	−1.20	−0.26
	221	20.	−2.06		−1.08	−1.38		−0.86
	1905	21.	−2.06	−0.80	−1.31	−1.38	−1.37	−0.68
	1457	22.	−2.04	−0.03	−1.23	−1.57	0.72	−1.02
	417	23.	−2.03		−0.84	−1.22		−0.96
	1328	24.	−2.01	−1.41	−1.19	−1.31	−0.65	-0.34
	545	25.	−2.00	−0.39	−2.49	−02.17	0.40	−0.94
	1641	26.	−2.00	−3.13	−2.17	−1.91	−1.42	−1.31
	1230	27.	−1.98	−1.78	−1.08	−1.54	−1.16	−0.38
	1129	28.	−1.94	−1.03	−1.47	−1.60	−0.05	−0.34
	1790	29.	−1.94	−1.77	−1.00	−1.36	−1.12	−1.08
	542	30.	−1.93	0.46	−3.07	−2.51	1.68	−1.77
Arithmetic mean			−2.27	−1.68	−1.41	−1.52	−1.00	−0.86
30 warmest years	933	1.	1.45	1.24	−0.12	0.07	1.40	0.20
	6	2.	1.46		0.42	−0.26		−0.40
	509	3.	1.46	1.20	−0.83	−0.91	0.61	−0.25
	747	4.	1.47	0.29	−0.85	−0.71	0.35	0.49
	509	3.	1.46	1.20	-0.83	-0.91	0.61	-0.25
	747	4.	1.47	0.29	-0.85	-0.71	0.35	0.49
	1019	5.	1.47	1.14	0.20	-0.15	1.43	0.16
	38	6.	1.48		0.44	-0.09		0.22
	45	7.	1.49		-0.01	-0.60		-0.20
	1092	8.	1.49	2.37	0.87	1.33	2.74	2.02
	79	9.	1.50		-0.43	-0.71		0.58
	406	10.	1.51		1.03	1.23		0.45
	49	11.	1.52		0.17	0.01		0.37
	27	12.	1.54		0.07	-0.40		-0.08
	37	13.	1.54		0.65	0.22		0.46
	483	14.	1.59		-0.45	-0.68		0.28
	4	15.	1.60		0.87	0.30		0.51
	43	16.	1.61		0.47	-0.37		-0.01
	47	17.	1.61		-0.11	-0.43		-0.39
	757	18.	1.63	1.95	-0.26	-0.35	2.84	0.02
	760	19.	1.70	2.02	-0.20	-0.42	2.70	-0.35
	837	20.	1.70	0.61	-0.57	-0.76	1.64	-0.23
	99	21.	1.72		0.13	-0.13		0.46
	507	22.	1.72	0.65	-1.22	-1.25	0.99	-0.61
	934	23.	1.72	2.12	0.29	0.63	2.67	0.57
	751	24.	1.73	0.58	-0.72	-0.69	1.62	-0.04
	1831	25.	1.77	2.23	1.07	0.74	2.22	0.27
	493	26.	1.82		0.52	0.30		0.12
	891	27.	1.96	1.40	-0.39	-0.09	2.59	1.01
	34	28.	1.97		0.44	-0.30		-0.11
	46	29.	2.07		0.27	-0.10		0.59
	1937	30.	2.09	2.14	0.59	1.22	2.00	1.78
Arithmetic mean			1.65	1.44	0.08	-0.11	1.84	0.28

temperature pattern. Since we here calibrated all reconstructions using the same method, between-record differences are likely related to varying data treatment and chronology development methods, measurement techniques, and/or sampling strategies, as well as the remaining uncertainty typical to such proxy data. For example, splicing of MXD data on recent TRW trends as done in Briffa92 might have caused this reconstruction to appear at the lower (colder) end of the ensemble, whereas the combination (and adjustment) of novel digital MXD measurements with traditional X-ray based MXD data as done in Grudd08 might have caused this reconstruction to appear at the upper (warmer) end of the ensemble. Other differences are likely related to the combination of sub-fossil material from trees that grew in

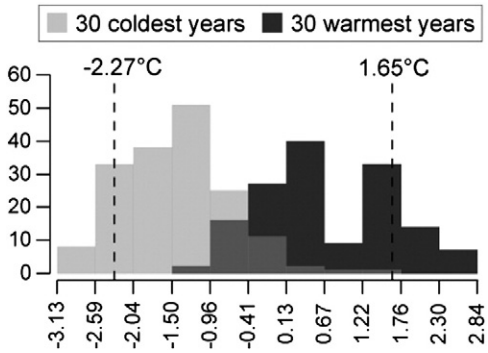

Fig. 9. Distributions of reconstructed extreme temperatures over the past two millennia. Light (dark) grey histogram shows the distribution of reconstructed JJA temperatures derived from six tree-ring based reconstructions in the 30 coldest (warmest) years of the N-Scan record (see Table 3). Overlapping values are shown in grey. Dashed lines indicate mean temperatures of the 30 coldest and warmest summers considering only the N-Scan reconstruction. All reconstructions were calibrated against regional JJA temperatures over the 1876–1993 period using OLS regression. Temperatures are expressed as anomalies in degrees Celsius from the 1951–1980 mean.

wet conditions at the lakeshores with material from living trees growing in dryer 'inland' sites. Also varying variance stabilization (Frank et al., 2007) and detrending techniques (Esper et al., 2003) in association with temporally changing sample replications and age distributions of the underlying data (Melvin, 2004) likely impacted the variance structure of the long-term records and consequently the absolute levels of reconstructed temperatures.

Between-reconstruction variance as revealed here represents a pending challenge for the integration of proxy records over larger regions and the development of a single timeseries that represents the Northern Hemisphere (e.g., Mann et al., 2008), for example. The composition of such records commonly relies on the calibration statistics derived from fitting regional proxy records against instrumental data (D'Arrigo et al., 2006). However, the records analyzed here would all easily pass conventional calibration-based screening procedures. Yet our analysis revealed that choosing one Scandinavian record instead of another one can alter reconstructed temperatures by 1.5-3 °C during Medieval times, for example. On the other hand, consideration of all records presented here would likely promote a less variable climate history, as the combination of diverging records tends to reduce variance in the mean timeseries (Frank et al., 2007). If such a mean is then combined with instrumental data covering the past 100–150 years, this approach might facilitate hockey stick-shaped reconstructions (Frank et al., 2010a). This seems to be a tricky situation in which expert teams including the developers of proxy records might need to be involved to help assessing timeseries beyond the typical ranking based on calibration statistics.

Our results showed that introducing an improved temperature reconstruction does not automatically clarify climate history in a given region. In northern Scandinavia, we now arrive at a situation where a number of high-resolution proxy records – all passing classical calibration and verification tests – are available within a confined region that is characterized by homogeneous temperature patterns. These records, however, differ by several degrees Celsius over the past two millennia, which appears huge if compared with the 20th Century warming signal in Scandinavia or elsewhere. We conclude that the temperature history of the last millennium is much less understood than often suggested, and that the regional and particularly the hemispheric scale pre-1400 temperature variance is largely unknown. Expert teams are needed to assess existing records, and to reduce uncertainties associated with millennium-length temperature reconstructions, before we can usefully constrain future climate scenarios.

Acknowledgements

Dani Nievergelt and Anne Verstege produced high-resolution density profiles at the WSL, Switzerland. Supported by the Mainz Geocycles Research Centre, and the European Union project Carbo-Extreme (226701).

References

Berger, A., Loutre, M.F., 1991. Insolation values for the climate of the last 10million years. Quaternary Science Reviews 10, 297–317.
Briffa, K.R., et al., 1992. Fennoscandian summers from AD 500: temperature changes on short and long time scales. Climate Dynamics 7, 111–119.
Briffa, K.R., et al., 2008. Trends in recent temperature and radial tree growth spanning 2000 years across northwest Eurasia. Philosophical Transactions of the Royal Society of London. Series B 363, 2269–2282.
Büntgen, U., et al., 2011. European climate variability and human susceptibility over the past 2500 years. Science 331, 578–582.
Cook, E.R., Kairiukstis, L.A., 1990. Methods of dendrochronology – applications in the environmental science. Kluwer Academic Publishers, Dordrecht, p. 394.
Cook, E.R., Esper, J., D'Arrigo, R., 2004. Extra-tropical Northern Hemisphere temperature variability over the past 1000 years. Quaternary Science Reviews 23, 2063–2074.
D'Arrigo, R., Frank, D., Jacoby, G., Pederson, N., 2001. Spatial response to major volcanic events in or about AD 536, 934 and 1258: Frost rings and other dendrochronological evidence from Mongolia and northern Siberia. Climatic Change 49, 239–246.
D'Arrigo, R., Wilson, R., Jacoby, G., 2006. On the long-term context for late 20th century warming. Journal of Geophysical Research 111, D03103. doi:10.1029/2005JD006352.
D'Arrigo, R., Wilson, R., Liepert, B., Cherubini, P., 2008. On the 'Divergence Problem' in Northern Forests: A review of the tree-ring evidence and possible causes. Global and Planetary Change 60, 289–305.
Eronen, M., Zetterberg, P., Briffa, K.R., Lindholm, M., Meriläinen, J., Timonen, M., 2002. The supra-long Scots pine tree-ring record for Finnish Lapland: Part 1, Chronology construction and initial inferences. The Holocene 12, 673–680.
Esper, J., Frank, D.C., 2009. Divergence pitfalls in tree-ring research. Climatic Change 94, 261–266.
Esper, J., Cook, E., Schweingruber, F., 2002. Low-frequency signals in long tree-ring chronologies for reconstructing past temperature variability. Science 295, 2250–2253.
Esper, J., Cook, E.R., Krusic, P.J., Peters, K., Schweingruber, F.H., 2003. Tests of the RCS method for preserving low-frequency variability in long tree-ring chronologies. Tree-Ring Research 59, 81–98.
Esper, J., Frank, D.C., Wilson, R.J.S., Briffa, K.R., 2005. Effect of scaling and regression on reconstructed temperature amplitude for the past millennium. Geophysical Research Letters 32. doi:10.1029/2004GL021236.
Esper, J., Frank, D.C., Büntgen, U., Verstege, A., Hantemirov, R.M., Kirdyanov, A.V., 2010. Trends and uncertainties in Siberian indicators of 20th century warming. Global Change Biology 16, 386–398.
Frank, D., Esper, J., 2005. Characterization and climate response patterns of a high-elevation, multi-species tree-ring network for the European Alps. Dendrochronologia 22, 107–121.
Frank, D., Esper, J., Cook, E.R., 2007. Adjustment for proxy number and coherence in a large-scale temperature reconstruction. Geophysical Research Letters 34. doi:10.1029/2007GL030571.
Frank, D., Esper, J., Zorita, E., Wilson, R., 2010a. A noodle, hockey stick, and spaghetti plate: a perspective on high-resolution paleoclimatology. Wiley Interdisciplinary Reviews: Climate Change 1. doi:10.1002/wcc.53.
Frank, D.C., et al., 2010b. Ensemble reconstruction constraints on the global carbon cycle sensitivity to climate. Nature 463, 527–530.
Gouirand, I., Linderholm, H.W., Moberg, A., Wohlfarth, B., 2008. On the spatiotemporal characteristics of Fennoscandian tree-ring based summer temperature reconstructions. Theoretical and Applied Climatology 91, 1–25.
Grudd, H., 2008. Torneträsk tree-ring width and density AD 500–2004: A test of climatic sensitivity and a new 1500-year reconstruction of north Fennoscandian summers. Climate Dynamics 31, 843–857.
Grudd, H., et al., 2002. A 7400-year tree-ring chronology in northern Swedish Lapland: natural climatic variability expressed on an- nual to millennial timescales. The Holocene 12, 657–665.
Hegerl, G., Crowley, T., Hyde, W., Frame, D., 2006. Climate sensitivity constrained by temperature reconstructions over the past seven centuries. Nature 440, 1029–1032.
Helama, S., Fauria, M.M., Miellikainen, K., Timonen, M., Eronen, M., 2010. Sub-Milankovitch solar forcing of past climates: Mid and late Holocene perspectives. GSA Bulletin 122, 1981–1988.
IPCC, 2007. Climate Change 2007. The Physical Science Basis. Cambridge Univ. Press, Cambridge, p. 996.
Jones, P., et al., 2009. High-resolution paleoclimatology of the last millennium: a review of current status and future prospects. The Holocene 19, 3–49.
Lee, T., Zwiers, F., Tsao, M., 2008. Evaluation of proxy-based millennial reconstruction methods. Climate Dynamics 31, 263–281.
Mann, M.E., et al., 2008. Proxy-based reconstructions of hemispheric and global surface temperature variations over the past two millennia. Proceedings of the National Academy of Sciences of the United States of America 105, 13252–13257.

Melvin, T., 2004. Historical growth rates and changing climatic sensitivity of boreal conifers. Ph.D. thesis, Climatic Research Unit, East Anglia, UK.
Schweingruber, F.H., 1988. Tree Rings: Basics and Applications of Dendrochronology. Kluwer Academic Publishers, Dordrecht, p. 276.
Schweingruber, F.H., Fritts, H.C., Bräker, O.U., Drew, L.G., Schaer, E., 1978. The X-ray technique as applied to dendroclimatology. Tree-Ring Bulletin 38, 61–91.
Yamazaki, Y.H., Allen, M.R., Huntingford, C., Frame, D.J., Frank, D.C., 2009. Refining future climate projections using uncertain climate data of the last millennium. Geophysical Research Abstracts 11 EGU2009-1204-2.